

# EXPERIMENTAL TESTS ON FRACTURE STRENGTH OF NANOTUBES

R. S. Ruoff<sup>1</sup>, L. Calabri<sup>2</sup>, W. Ding<sup>1</sup> and N. M. Pugno<sup>3</sup>

<sup>1</sup>Department of Mechanical Engineering, Northwestern University, Evanston, IL 60208-3111, USA

<sup>2</sup>Dipartimento di meccanica e tecnologie industriali, Università di Firenze, Via di Santa Marta 3, 50139, Firenze, Italy

<sup>3</sup>Department of Structural Engineering, Politecnico di Torino, Corso Duca degli Abruzzi 24, 10129, Italy

Received: May 10, 2005

**Abstract.** A new experimental and post-analysis procedure to perform tensile-loading experiments on nanofibers, e.g., carbon nanotubes (CNTs) or nanowires, is presented. The procedure has been applied to multiwalled carbon nanotubes (MWCNTs). At this time, we consider the corresponding results on fracture strength (strain and Young's modulus) as preliminary, but these preliminary results strongly suggest the presence of defects in the tested nanotubes. Assuming defects like clusters of adjacent vacancies (e.g., atomistic blunt cracks) we tried to rationalize the preliminary experimental data by applying Quantized Fracture Mechanics (QFM). So far the experimental results are not sufficient to validate this approach, and the next step of this research is to obtain much more data, using our new methodology, to further test QFM, including possibly introducing atomistic defects of well-known size and shape in a controlled way.

## 1. INTRODUCTION

Uniaxial nanostructures, e.g., nanotubes, nanowires and nanofibers, have recently stimulated ever-broader research activities in science and engineering due to the promise of applications in sensing, materials reinforcement, vacuum microelectronics, and microelectromechanical or nanoelectromechanical systems.

New tensile testing methods have been developed to study the mechanical properties of nanostructures. The uniaxial tensile test is the most popular method for bulk material mechanical property characterization and it also is used in mechanical property measurements of nanostructures such as carbon nanotubes [1]. During tensile testing, an increasing tensile load is applied to a fiber until it

fractures. The specimen elongation and applied load is measured during the tensile loading process. The load might be applied continuously or in increments. With the tensile test data, the modulus of elasticity, tensile strength, elongation and other tensile properties of the material are determined, if the geometry of the specimen is well known.

Recently, we performed tensile testing experiments on arc-grown multi-walled carbon nanotubes (MWCNTs; MER Corp. AZ, USA). The primary arc-grown material consists of powdered cathode deposit (core material) with 30-40% MWCNT content and other graphitic particles. Fig. 1 shows SEM images of this MWCNT material. The supplier (MER Corp.) states that the MWCNTs have 8-30 layers, are 6-20 nm in outer diameter and 1-5 microns in length.

---

Corresponding author: R. S. Ruoff, e-mail: r-ruoff@northwestern.edu

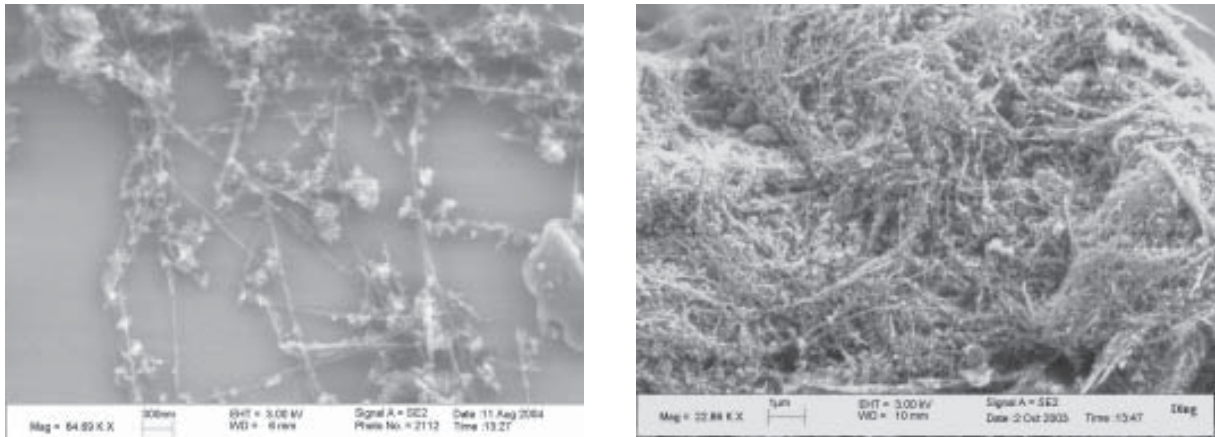


Fig. 1. SEM images of MWCNTs powder source from MER Corp.

## 2. EXPERIMENTAL PROCEDURE

A droplet of MWCNTs dispersed in ethanol was put on a plasma-cleaned silicon substrate. After the ethanol evaporated, MWCNTs remained on the surface, together with some small particles. Then, a TEM grid that had been cut in half was used to 'scratch' MWCNTs from the substrate. This TEM grid, with MWCNTs attached at the ledge, served as the nanotube source for tensile tests. Fig. 2 shows examples of MWCNTs at a ledge of a TEM grid, ready for pick up with AFM tips to perform tensile testing.

The tensile testing experiments were performed inside a LEO 1525 field emission gun SEM with our home-built nano-manipulator [2]. This manipulator is composed of two separate stages, namely a X-Y linear motion stage and a Z linear motion stage. Two AFM cantilevers were attached to these two opposing stages: (i) a soft one (CSC 12

MikroMasch, 350 microns, nominal force constant 0.03N/m) to the X-Y stage, which is itself attached to a piezo bender (Noliac A/S, Denmark, ceramic multiplayer bender B1), and (ii) a rigid one (NSC12 MikroMasch, 90 microns, nominal force constant 14N/m) that is attached to the Z linear motion stage. The MWCNT source was attached to the Z stage.

During the experiment, a MWCNT was clamped to the soft cantilever tip via electron beam induced deposition (EBID). Then, the MWCNT was picked up from the source, and the other end of the MWCNT was clamped to the tip of the rigid cantilever with EBID clamping. Fig. 3 shows an individual MWCNT clamped between two AFM cantilever tips. Due to the small dimension of the MWCNT, high magnification is needed in order to measure the cantilever deflection and tube elongation during tensile loading.

During the experiment a tensile force was applied to the MWCNT through the cantilever deflec-

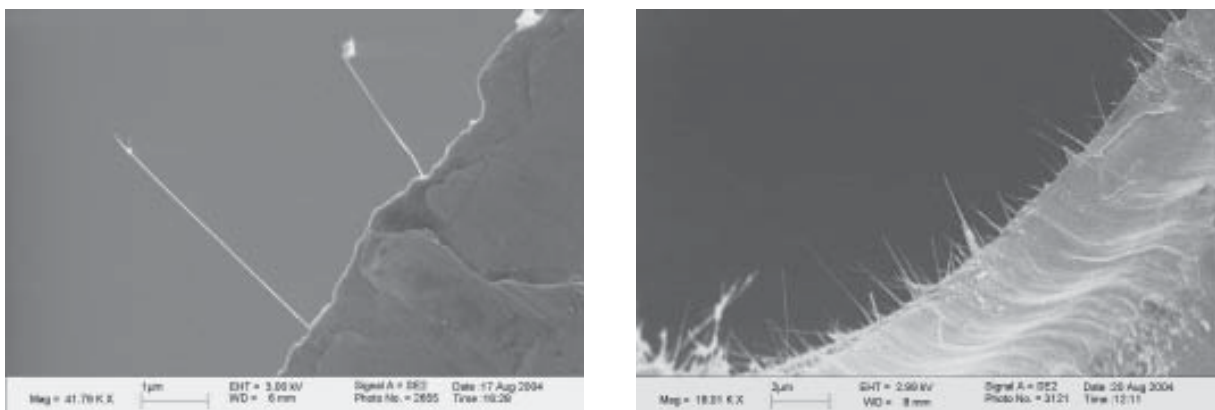
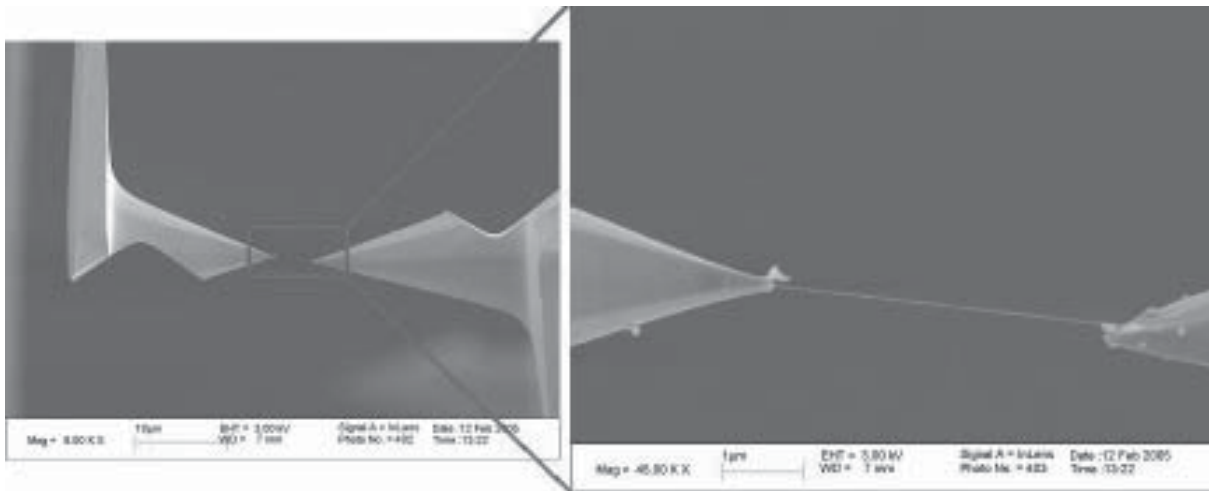


Fig. 2. Protruding MWCNTs at the ledge of part of a TEM grid.



**Fig. 3.** SEM images of a tensile test on an individual MWCNT. The dark material on the AFM cantilever tip surface is paraffin we deliberately deposited, to increase the speed of EBID clamping.

tion, which was induced by the controllable bending of the piezo bender with a DC bias. Eventually the MWCNT fractured with increasing tensile load; typically, MWCNTs failed in the sword-in-sheath manner [1] (Fig. 4). From SEM images, the cantilever deflection was obtained, and the corresponding tensile force was calculated. The elongation of the MWCNT was also measured from the SEM images. With the knowledge of the MWCNT dimension, the Young's modulus and fracture strength of the MWCNT were evaluated.

Due to the small size of the MWCNTs, it is challenging to achieve a precise measurement on the MWCNT diameter inside the SEM. Therefore the MWCNT fragments remaining on each AFM tip following fracture were individually transferred to TEM for observation. A special TEM holder was used to hold the AFM cantilever in the vertical position to

enable imaging of the attached nanotube. Fig. 5 shows SEM and TEM images of a fractured MWCNT segment.

### 3. POST-ANALYSIS PROCEDURE

Fig. 3 shows an overview of a tensile-loading experiment. In this case the structure analyzed is a MWCNT, so its dimensions are really small; in fact it's necessary to 'zoom in' the space between the two cantilevers to have a clear image of it.

The goal of this type of test is to characterize the mechanical behavior of the MWCNTs, thus to obtain its breaking strength and Young modulus, and in general its stress-strain response curve.

For calculations, it is necessary to precisely determine the forces acting on the MWCNT during the test, and to accurately measure its elongation

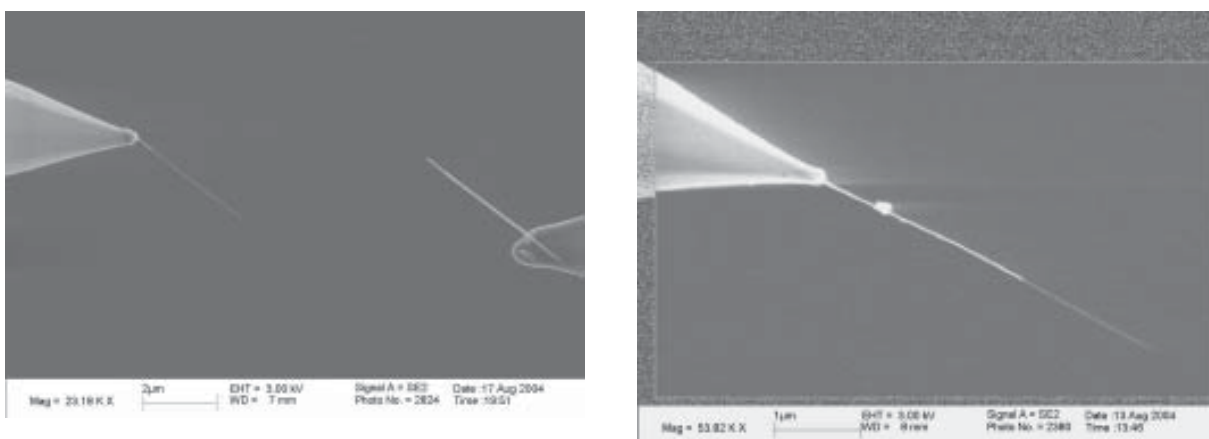


**Fig. 4.** The sword-in-sheath failure examples of MWCNTs during tensile test.

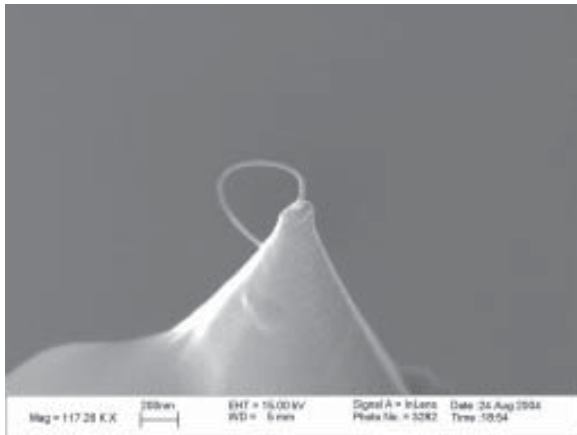
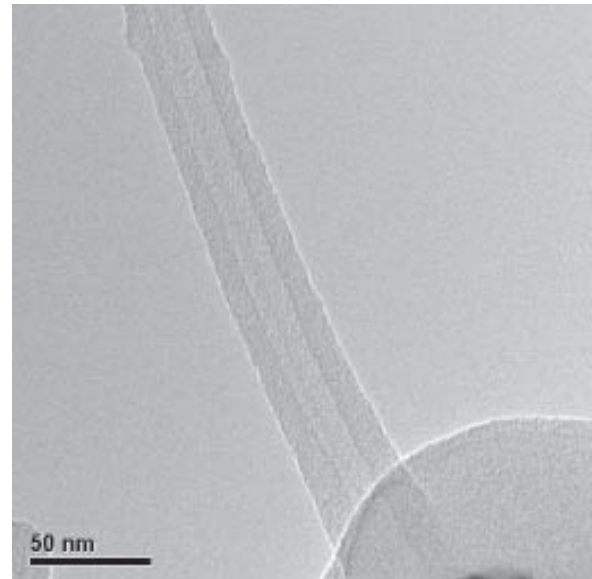


**Fig. 5.** SEM (left) and TEM (right) images of a fractured MWCNT attached to AFM tip.



(to fit the Young’s modulus). There are several methods to evaluate the forces and elongations, but all of them are based on the analysis of the SEM images taken during the tensile loading process. For these particular MWCNTs (arc grown) the length is small enough, e.g., 1-5  $\mu\text{m}$ , that it is non-trivial to properly configure the experiment to be able to carry out a high-quality tensile testing with consistent results.

#### 4. STRAIN-STRESS CURVE

**Force Measurement.** The outline in Fig. 6 shows an overview of the tensile-loading experiment. In the

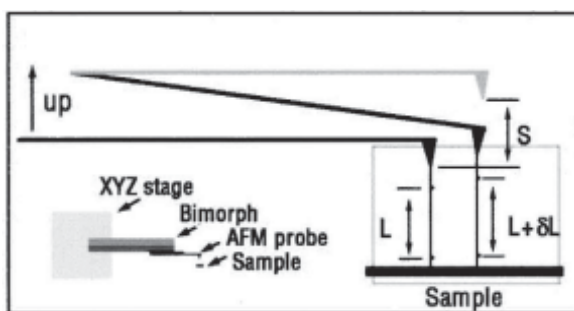


**Fig. 6.** Schematic showing the principle of the tensile-loading experiment. The cantilever is driven upward and it bends downward by a tip displacement  $S$ , while the nanotube is stretched from its initial length of  $L$  to  $L + \delta L$  because of the force exerted on it by the AFM tips. The force is calculated as  $k\delta L$ , where  $k$  is the force constant of the cantilever. The strain of the nanotube is  $\delta L/L$ .

schematic, the grey cantilever indicates where the cantilever would be if no tube were attached on the AFM tips [3].

To determine the forces acting on the MWCNT, an image processing method has been used. By knowing the displacement  $S$  (Fig. 6) of the cantilever it is possible to calculate the force acting on the MWCNT, simply by multiplying the displacement  $S$  by the force constant  $k$  of the cantilever. Thus, to calculate accurately the force we need to measure precisely the displacement  $S$ .

In this particular case it was not possible to measure directly the displacement  $S$  from the image, as we could see only the tip of the bent cantilever (Fig. 3). In order to measure the displacement, there must be a static reference point on the image (often it is possible to use an unbent cantilever on the same chip, similar to the grey cantilever seen in the schematic).

Being unable to use a reference point to track the cantilever deflection (that is a future goal—to have such an internal reference present), we employed a new method based on the angle of deflection  $\alpha$  of the cantilever (Fig. 7). With this method, it is quite simple to obtain good results without a reference.

Measuring the variation of the cantilever angle step by step, one can determine the force  $F = 2/3(\alpha Lk)$ , where  $\alpha$  is the angle of deflection (Fig. 7) and  $L$  the cantilever length. The force constant  $k$  is a parameter unique to each cantilever, so it is necessary to evaluate this parameter for each with a dynamic test (Sader method [4,5]). By measur-

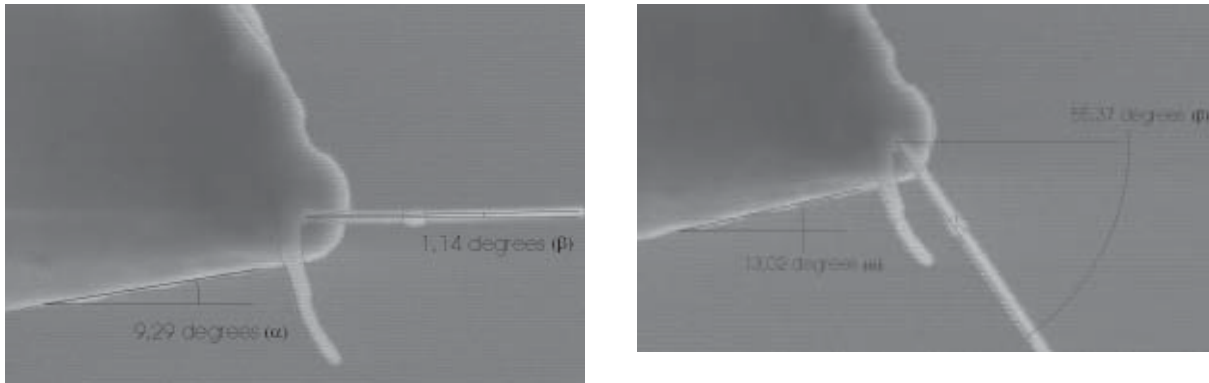


**Fig. 7.** Sequence of template SEM images of a tensile test on an individual MWCNT.

ing the oscillation fundamental frequency  $f$  of the cantilever it is possible to obtain its force constant using the following formula  $k=M\rho bhLf^2$ , where  $b$  and  $h$  are the cross-section cantilever dimensions,  $\rho$  is the cantilever mass density and  $M$  is the normalized effective mass.

To properly measure the angle of deflection of the tip, it is important to always use exactly the same edge of the cantilever at each step. Oftentimes, it is difficult to obtain a high resolution image of the tip, so to ensure that we are always using the same edge, we have used distinctive features on the tip to create a reference on the image (see the red template on the tip, Fig. 7).

The force  $F$  obtained as described, is theoretically applied axially along the tip. However, the nanotube is not always aligned perfectly along the tip, so an angle correction is necessary to obtain the axial load, i.e.,  $F=F\cos\beta$ , where  $\beta$  is the angle between the tube and the axis of the tip (Fig. 7).

Another way to measure the displacement  $S$  of the cantilever is by using the bimorph response. The dependence of the deflection  $S_0$  of the AFM tip as a function of applied voltage to the bimorph was independently determined in the absence of any attached specimen (bimorph calibration – Fig. 8). So, while the MWCNT is being stretched due to application of a given voltage to the bimorph, the AFM tip position change,  $\delta L$  (Fig. 6), is calculated using the image analysis. The true deflection of the AFM cantilever is  $S=S_0-\delta L$ .

**Elongation measurement.** Fig. 9 shows the image analysis used to measure the tube elongation. The concept is quite simple, and requires measuring the length of the tube and its variation step by step. Unfortunately, the resolution of the images (at very high magnification) does not allow for sufficiently

accurate evaluation. For this reason we have used the same method as for the force measurement. In fact a reference on each of the tips is used to know exactly the position of the clamps. Since the reference should remain at the same point during each step of the process, it is possible to measure the length of tube step by step.

To obtain better results, it is recommended to use, if possible, references directly on the MWCNT (distinctive features on it, e.g., particles). In this particular test it is possible to see two particles on the nanotube.

The units showed on the images (mm) are merely the units that the image-software uses to analyze the pictures, but they have been converted to the real units (nm) using the scale bar presented in each picture (Figs. 1-5).

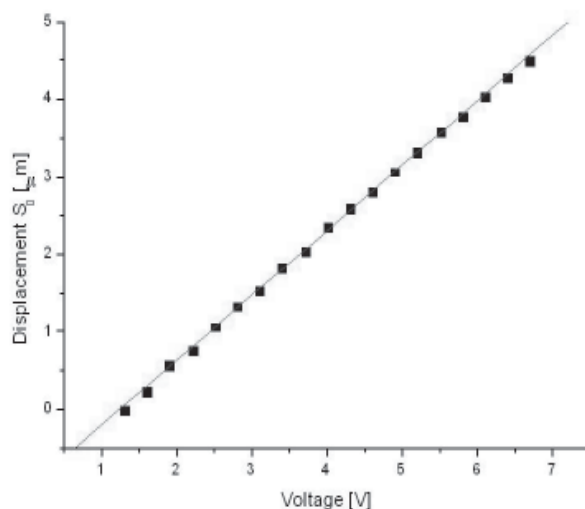


**Fig. 8.** Bimorph calibration: dependence of the deflection  $S_0$  of the AFM tip as a function of applied voltage to the bimorph.

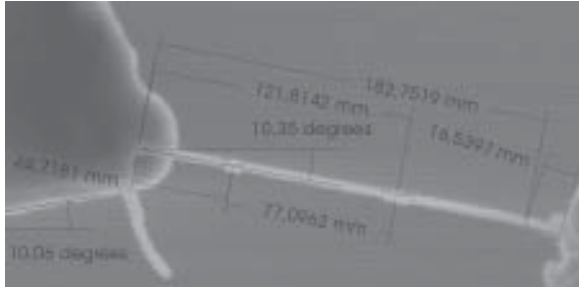


**Fig. 9.** Template SEM image of a tensile test on an individual MWCNT.

### 5. PRELIMINARY RESULTS AND QFM COMPARISON

In this experimental study several arc-grown MWCNTs have been tested, but at this time we only have preliminary results to report. Here, as an example, we report on the preliminary results for one of the most interesting cases, sample 08-08 #4 MWCNT.

Table 1 lists the experimental result for this MWCNT based on the cantilever deflection angle. Since the MWCNT was fractured in the sword-in-sheath manner, we assume that only the outermost shell was fractured. We have taken the resistant area of the outer shell as the area of an annulus with a thickness of 0.34 nm. The measured strength is 49.4GPa. To confirm this result, we considered the force determined from the bimorph calibration, and we obtained the value reported in Table 2, i.e., 45.7 GPa.

If we assume adjacent vacancies orthogonal to the applied tensile load (the orthogonal condition is the most critical) as the critical defect in this MWCNT we can derived the length of the corresponding atomistic blunt crack in unity of fracture quanta (the distance between two adjacent chemical bonds, i.e., for nanotubes  $\sqrt{3}$  times the interatomic distance) according to Quantized Fracture Mechanics (QFM) [6]. Assuming an ideal strength of 93.5 GPa, as computed by Molecular Mechanic (MM) atomistic simulations (see [3]) and a tip radius of 2 Angström, as fitted in [3] from the MM simulations, the crack length in unit of fracture quantum corresponding to 49.4GPa is computed as  $n=4$ . Thus, just 4 adjacent vacancies are expected to give a strength reduction compatible with the observation. Note that a nanotube with radius of 10 nm (ours have outermost layers having diameters of 6-20 nm) would have

**Table 1.** Results for the 08-08 #4 MWCNT sample based on cantilever angle measurement.

Deflection ( $\alpha$ )	Force [ $\mu$ N]	Area [ $\text{nm}^2$ ]	Breaking Strength [GPa]
2.19°	1.06	21.36	49.4

**Table 2.** Results for the 08-08 #4 MWCNT sample based on bimorph displacement calibration.

Force [ $\mu$ N]	Area [ $\text{nm}^2$ ]	Breaking Strength [GPa]
0.98	21.36	45.7

**Table 3.** Strain between different marks.

Sketch	Initial length [ $\mu$ m]	Elongation [ $\mu$ m]	Strain (%)
A-D	1.81	0.190	10.47
A-B	0.41	0.036	8.71
B-C	0.71	0.047	6.71
A-C	1.12	0.083	7.42

a circumference of length  $n \sim 250$  atoms; thus, even a very small cross-section reduction can cause a tremendous strength reduction, as pointed out in [3].

For the displacement, as shown in Fig. 10 (left), we analyzed four cases in this experiment: the elongation throughout the whole tube between points A-D, between A-B, B-C or A-C. The strain results were obtained based on distance measurements among these different marks as shown in Table 3.

With the knowledge of the strain and corresponding stress, we can plot a stress-strain curve. And by determining the slope of the curve, the Young's modulus of the MWCNT can be obtained. Fig. 10 (right) shows an example of stress-strain curve for the MWCNT based on the strain measurement B-C.

With the data analysis method we discussed above, we analyzed all the tensile tests we have collected to date, but our experimental work continues (Table 4).

**Table 4.** MWCNT tensile testing results and QFM interpretation assuming blunt cracks adjacent vacancies. Testing between 2 AFM tips (or AFM tip and TEM grid\*).

Sample	Length [ $\mu\text{m}$ ]	Diameter [nm]**	Breaking Strength [GPa]	Crack length (QFM) – n	Young's Modulus [GPa]
08-03 #1*	6.1	20	15.0	54	81
08-08 #1*	1.2	20	6.0	(341)	36
08-08 #4 (A-D)	1.8	20	49.4	4	427, 517, 537, 559
08-10 #1 (A-C)*	1.95	20	17.6	39	495, 482, 427
08-10 #2	1.0	20	44.4	5	450

\*\*Diameter is simply assumed as equal to 20 nm (their correct values will be measured in the future in TEM imaging).

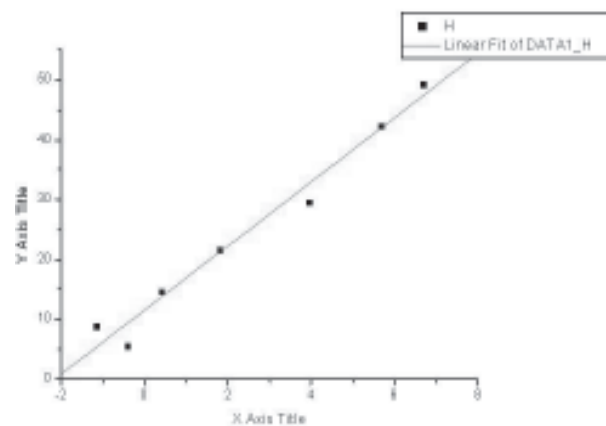
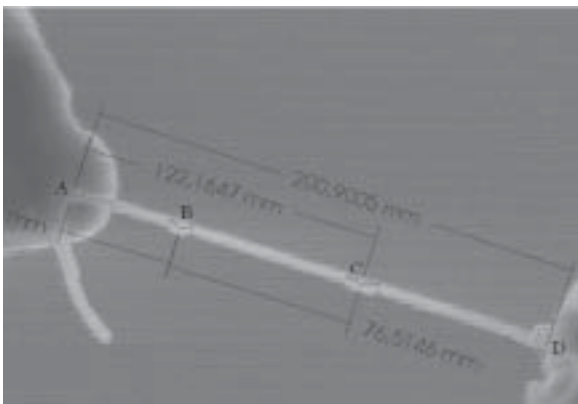


**Fig. 10.** The strain measurement with internal marks. Points A, B, C, and D are marks on the tube that were used to evaluate the strain in different section of the tube (left). The stress (Y axis)-strain (X-axis) relationship of the 08-08 #4 MWCNT sample, based on the strain measurement B-C (right).

## 6. CONCLUDING REMARKS

The proposed experimental and post-analysis procedure and Quantized Fracture Mechanics should be useful tools in the study of fracture strength at nanoscale. The preliminary results about the nanotube testing seem to confirm the availability of the QFM method on predicting the fracture strength of nanostructures. But the limited number of experiments and the difficulty in measuring the nanostructure dimensions, especially the nanotubes diameter, shows that more work is clearly needed. With this new experimental and post-analysis procedure it is possible to perform experiments with a methodological approach, so to apply this process to each kind of uniaxial nanostructure.

## ACKNOWLEDGEMENTS

We gratefully acknowledge the grant support from the NSF grant 'Mechanics of Nanoropes' (NSF #0200797, Ken Chong program manager), and the NSF grants NIRT: Electrical and Mechanical Properties of Boron and Metal and Nanoscale Devices Built from them (NSF #0210120) and NIRT: Synthesis, Characterization and Modeling of Aligned Nanotube Arrays for Nanoscale Devices and Composites (NSF #030450); and from the Office of Naval Research 'Mechanics of Nanostructures' grant under award No. N000140210870 and the NASA University Research, Engineering and Technology Institute on Bio Inspired Materials (BIMat) under award No. NCC-1-02037.

## REFERENCES

- [1] M.F. Yu *et al.* // *Science* **287** (2000) 637.
- [2] M.F. Yu *et al.* // *Nanotechnology* **10** (1999) 244.
- [3] D. Qiang *et al.* // *Appl. Mech. Rev.* **55** (2002) 495.
- [4] J. E. Sader *et al.* // *Rev. Sci. Instru.* **70** (1999) 3967.
- [5] J. E. Sader *et al.* // *Rev. Sci. Instru.* **66** (1995) 3789.
- [6] N. Pugno and R. Ruoff // *Phil. Mag.* **84** (2004) 2829.